

PLANNING ALGORITHMS FOR INDOOR ROBOTIC ODOR LOCALIZATION

Final Report

16.622

Fall 2012

Authors:

Troy Astorino

Mark Van de Loo

Advisors:

Professor Youssef Marzouk

Professor Nicholas Roy

Josh Joseph

Javier Velez

Xun Huan

Sachi Hemachandra

December 12, 2012

Abstract

A greedy gradient descent planning algorithm and a stochastic planning algorithm were compared in the context of indoor robotic odor localization. A ground robot was equipped with an electronic nose that uses metal oxide sensors to measure chemical concentration. State estimation was implemented through the use of a particle filter that assumed a chemical concentration profile exponentially decaying with the square of the distance to the source. In localizing a single chemical vapor source in a closed room, there was not shown to be a statistically significant difference between the localization rates achieved by the two planners. It is concluded that further research in the area of modeling and estimation techniques for indoor robotic odor localization is necessary, and potential avenues for future work are discussed.

Contents

Contents	2
List of Figures	4
List of Tables	5
I Introduction	6
II Hypothesis, Objective, Success Criteria	6
III Literature Review	7
A Experiment Motivation	7
B Selection of Model and Estimator	7
C Selection of Planners	8
IV Description of Experiment	8
A Experimental Overview	8
B Test Apparatus	9
1 Hardware and Robot Platform	9
2 System Control Flow	10
3 Estimator	11
4 Planner	12
C Experimental Process	13
1 Test Environment	13
2 Test Procedure	13
3 Data Acquisition	14
V Results	15
A Experimental Data	15
B Statistical Hypothesis Assessment	15
C Additional Assessment of Results	16
VI Discussion	16
A Future Work	20
VII Summary and Conclusion	22
VIII Acknowledgments	22

References	23
-------------------	-----------

A Additional Figures	24
-----------------------------	-----------

List of Figures

1 Alpha MOS NEEM chemical sensor.	9
2 Envoy robotic wheelchair platform with Alpha MOS Neem Sensor.	9
3 Data acquisition flowchart	10
4 Fit of model parameters to preliminary data.	12
5 Testroom floorplan and chemical vapor source locations.	13
6 Graphical representation of data and hypothesis.	16
7 Final posterior estimates for source locations 7 and 8	18
8 Final posterior estimates for all trials	24

List of Tables

1 Estimator parameters	11
2 Measurement model height offsets.	12
3 Parameters of the experiment.	14
4 Experimental Data	15
5 Student's t-test on probability mass increase inside localization radius.	17
6 Fraction of possible area covered by the different planning algorithms.	17
7 Probabilistically weighted distance from the posterior estimate to the source location	19
8 Kullback-Leibler divergence of the final particle filter posterior distribution from an 'ideal' Gaussian posterior distribution .	20

I. Introduction

Robotic odor localization¹ has real-world applications such as searching for a chemical leak in a factory or laboratory, or locating survivors of a natural disaster amidst the rubble of collapsed buildings. These applications require an odor localization robot to operate autonomously in an indoor environment. Indoor air currents caused by factors such as ventilation and air circulation systems, moving people or machinery, convection, and drafts from the outdoors represent a challenge in the localization of a chemical vapor source, since these effects may become dominant over diffusion and are unpredictable.

The purpose of this experiment was to explore the possibility of utilizing a probabilistic approach to robotic odor localization to mitigate the uncertainty introduced in the behavior of a chemical vapor plume by indoor air currents. Probabilistic approaches to robotic odor localization may be analyzed as a combination of three components: a model, an estimator, and a planner. The model is a mathematical function that describes the spatiotemporal variation of the chemical concentration. The estimator represents the process by which measurements of the chemical concentration are combined with the model in real time to obtain an estimate of the location of the chemical source. The planner is an algorithm that decides the location of the next measurement given the current estimate of the source location.

The goal of this experiment was to compare two different planners, a greedy gradient descent planner and a stochastic planner, while using the same estimation algorithm. No statistically significant difference was shown between the performance of the two planners.

II. Hypothesis, Objective, Success Criteria

Hypothesis

The mean localization rate of a 35-minute two-dimensional search by an autonomous ground robot equipped with a chemical vapor sensor will be 20 percent greater using a stochastic planner than using a greedy gradient descent planner.²

Objective

Equip a ground robot furnished by the CSAIL Robust Robotics Group with an Alpha MOS NEEM chemical sensor, implement the planners on the robot's software platform, and assess the mean localization rate of a cup of ethanol in a closed room.

¹Odor localization is defined as “the act of finding the location of a volatile chemical source in the environment.”[1]

² The greedy gradient descent algorithm always moves the robot in the direction of the best source estimate. A stochastic algorithm moves to a location randomly sampled from the source estimate probability distribution, allowing the planning algorithm to gain a more complete representation of the search space, at the potential cost of taking some unnecessary measurements.

Success Criteria

Determine the difference in mean localization rate to a sufficient precision such that the hypothesis can be assessed.

III. Literature Review

Review of previous work in the field of robotic odor localization helped to select this experiment's test environment of a windless indoor room. In addition, it provided the basis for the selection of a Bayesian inference estimator and a Gaussian model as parameters of the experiment, and motivated the selection of a greedy gradient descent planner and a stochastic gradient descent planner as interchangeable parts of the localization algorithm to be compared for speed.

A. Experiment Motivation

Robotic odor localization experiments have been conducted using chemical dispersion in water, air, and soil.^[1] In water and soil, diffusion is the dominating method by which a chemical emanates from a source and disperses through space. In air, where the Reynolds number is higher than in water or soil, the behavior of the chemical concentration is affected by the presence of turbulence in addition to chemical diffusion.^[1] This turbulence has led most robotic odor localization researchers to introduce an artificial wind source when working in air. This negates the effect of the turbulence, producing a concentration plume that behaves as a 2-dimensional Gaussian function in planes normal to the wind direction, and downwind of the source. ^[2] While smoothing the concentration field in this manner makes the task of locating the chemical source more straightforward, this environment is not representative of a realistic indoor scenario. A few experiments, such as that done by Ferri, et al., have been conducted in an indoor environment without an artificial wind source. ^[2] In general, however, it seems that turbulent indoor environments have been less explored than their artificial wind source counterparts. For this reason, it was decided that this experiment would be conducted in an ambient, windless indoor environment.

B. Selection of Model and Estimator

Due to the varying effects of turbulence and diffusion discussed in section 3.1, accurate modeling of the concentration field is dependent upon the medium and environment in which the experiment is conducted. However, many robotic odor localization researchers chose not to use a high-fidelity model of the concentration field, deeming this level of complexity unnecessary. ^[1] Most commonly used was a dispersion model based on a Gaussian function. Time invariant Gaussian models were used successfully in experiments in water and soil, as well as in air with an artificial wind source. ^[1] In turbulent air, Ferri, et al. successfully used a time invariant monotonic function with a single peak at the source location as a concentration model. ^[2] The two algorithms tested

both successfully localized a dish of ethanol in a mean time of less than 10 minutes, beginning an average distance of 1.8m from the source. The model used in these localization algorithms is not explicitly described in [2], but the assumption that the model is time invariant and monotonic with a single peak is a defining component of the successful localization algorithms presented in this paper. Based on the success of Ferri, et al., it was deemed reasonable to choose a Gaussian concentration model for this experiment, and to treat the effects of turbulence in the air as noise. A Bayesian estimation technique was selected to account for this noise in determining a probability distribution over the potential source locations after each measurement. Bayesian estimation is a common technique used in robotic localization and is described in [3].

C. Selection of Planners

Planners that were shown to be effective in turbulent air environments were mainly derived from observations of the behavior of biological organisms. [2] For example, Ferri et al. attempted to mimic the circling behavior of the Luna Moth in its search for a mate in one planner, and the weighted random walk exhibited by the chemotaxis of the E. coli bacterium in another. [2] No documentation of greedy gradient descent using a single sensor or other simple statistically motivated planners as applied to robot odor localization was found. Using greedy gradient descent is attractive because of its simplicity, but due to the turbulent nature of ambient indoor air, a greedy gradient descent planner may be prone to confusion by temporary local maxima of the chemical concentration. An alternative planner that may perform better in the turbulent environment without requiring a complicated model is based on stochastic gradient descent, which adds randomness to the gradient vector when prescribing the direction of motion. [4] This randomness may help avoid the issues caused by temporary local maxima.

IV. Description of Experiment

A. Experimental Overview

A greedy gradient descent planning algorithm and a stochastic planning algorithm were tested using the same measurement model and estimation algorithm. A sensor capable of identifying the concentration of ethanol in the surrounding air was mounted on a ground robot. A dish of ethanol was placed in a test room, and the mean rate at which the robot localized the ethanol source using the greedy planner was compared to the mean rate using the stochastic planner.

B. Test Apparatus

1. Hardware and Robot Platform

The Alpha MOS NEEM chemical sensor shown in Figure 1 was attached to the Envoy robotic platform of the Robust Robotics Group, illustrated in Figure 2. The sensor was mounted 30 cm above the ground.

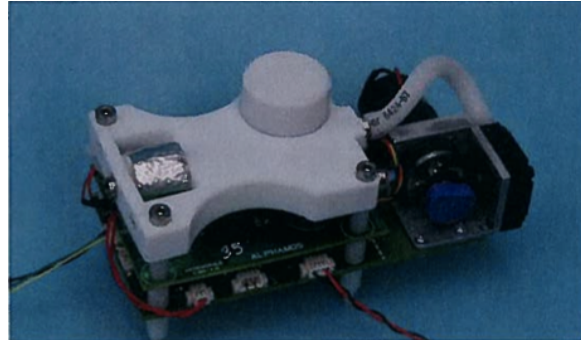


Figure 1. Alpha MOS NEEM chemical sensor.

A laptop computer mounted on the robot performed all real-time computation and data collection. The robot used two LIDARs and a pre-loaded map of the test room to determine its position. The robot's position was made available as telemetry to the estimator via the LCM messaging protocol at a rate of 40 Hz as illustrated in Figure 3.

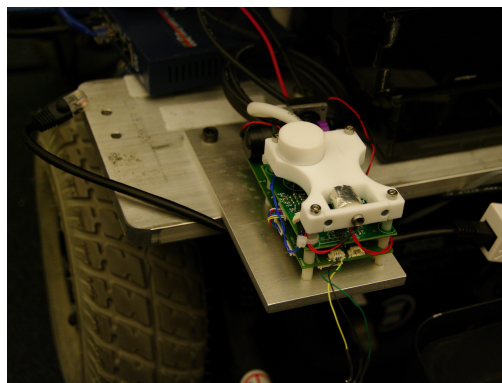


Figure 2. Envoy robotic wheelchair platform with Alpha MOS Neem Sensor.

2. System Control Flow

After reaching each measurement location commanded by the planner, the robot entered a waiting period of 30 seconds to allow transient concentration behaviors and sensor dynamics to attenuate before beginning to take readings. This period was followed by another 30 second period during which readings of the chemical vapor concentration were recorded at a rate of 1 Hz. These readings were averaged, and the natural logarithm of the average was passed to the estimator. An average reading was used because it was observed that there was a variance in the readings measured at any given location on the same order of magnitude as the average reading value. The estimator then used this value and the current position of the robot to update its posterior belief. This belief was passed to the planner, which commanded the next measurement location to the robot. The robot moved to that location and began the process again. Data flow between the components of the system is illustrated in Figure 3.

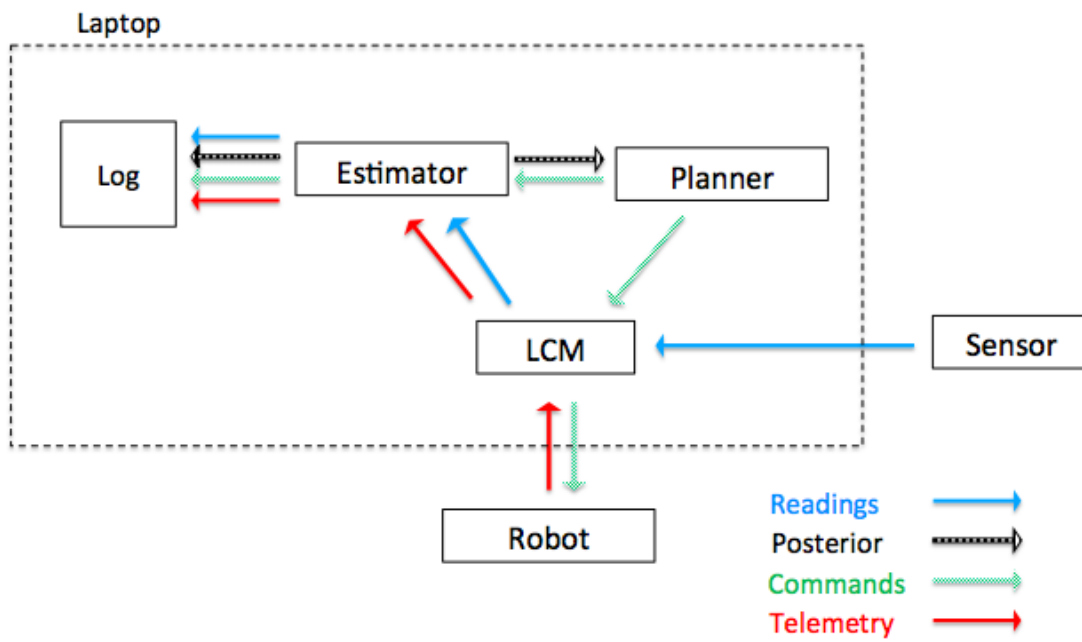


Figure 3. The components of the system, and the paths along which data is communicated. Messages are passed among different components of the robot's software using the LCM protocol. Sensor readings consist of a raw chemical concentration value. The posterior distribution is the robot's current best estimate of the chemical source's location. Commands are sent in the form of a target position and orientation of the robot. Telemetry includes the robot's position, velocity, and attitude.

3. Estimator

The estimate of the source location was calculated using a particle filter[5]. The particles were distributed with uniform spacing over the area of the test room, and each particle held the posterior estimate's belief that it was the location of the source. The particle density used is given in Table 1.

Each time the estimator received a measurement, a Bayesian update was performed on each particle as follows:

$$P_n(x_i = x_s) \propto P(c_n|x_i = x_s)P_{n-1}(x_s = x_i)$$

In the above expression, $P_n(x_i = x_s)$ represents the posterior belief that the source is located at the i^{th} particle location after the n^{th} update. x_i represents the position of the i^{th} particle, x_s represents the position of the source, and c_n represents the n^{th} measurement received by the estimator. $P(c_n|x_i = x_s)$ is the likelihood function, the probability that the measurement is equal to c_n given that the source is at the i^{th} particle location according to the measurement model. The measurement model assumes concentration measurements to be normally distributed according to:

$$c \sim \mathcal{N}(\bar{c}(x_s, x_r), \sigma)$$

$$\bar{c}(x_s, x_r) = q \exp\left[-\frac{|x_r - x_s|^2}{\nu^2}\right] + k$$

where x_r is the robot's location when the measurement is taken. The parameter values σ , q and ν were fitted from preliminary concentration data. The preliminary data and the fitted curves are presented in Figure 4, and the parameters of these fitted curves are shown in Table 1. Because the baseline chemical sensor reading was observed to vary across the preliminary trials, the height offset k was calculated by measuring the average baseline sensor readings over a period of 60 seconds before each trial began. The computed height offsets for all trials are listed in Table 2.

This simple measurement model does not consider asymmetric diffusion, time variation of diffusion, convection and wind currents, or the dynamic response of the sensor, all of which may have been present as disturbances in the test environment. It was believed that the estimation technique would cause the posterior estimate to accurately converge to the true source location by treating the deviations of real-world dynamics from the simple model as measurement noise.

Table 1. Particle filter and measurement model parameters.

Particle density	69.4 $\frac{\text{particles}}{\text{m}^2}$
σ	1.0
q	0.3748
ν	1.085
k	-10.8534

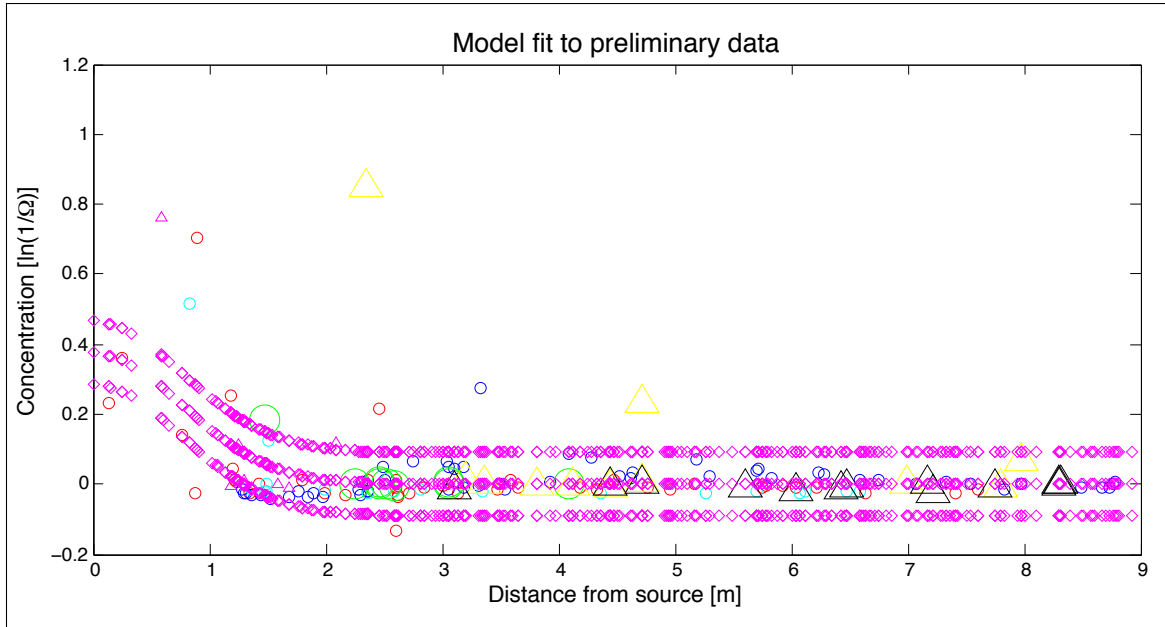


Figure 4. The fit of the measurement model to preliminary data. The purple diamonds show measurement models for different sets of trial data. The Alpha Mos NEEM sensor had different baseline concentration values on different days, so the measurement model used a height offset dependent on the baseline concentration on a given day. The other markers represent actual measured concentrations. The markers that are the same shape and color are from the same trial.

Table 2. Measurement model height offsets.

Height offset k	1	2	3	4	5	6	7	8	9
Greedy	-10.7078	-10.8031	-10.6224	-10.8217	-10.7253	-10.5972	-10.3781	-10.5596	-10.8351
Stochastic	-10.7088	-10.5289	-10.7939	-10.7022	-10.7959	-10.9099	-10.4587	-10.5746	-10.9096

4. Planner

This experiment compared a greedy gradient descent planning algorithm and a stochastic planning algorithm. The greedy algorithm always chose the next measurement location 1.5 m away from the robot's current position, in the direction of the maximum probability estimate of the source location. The maximum probability estimate was calculated by taking the weighted average of all of the estimator particle locations:

$$\hat{x}_s = \sum_i x_i P(x_s = x_i)$$

The stochastic planner sampled a random particle from the posterior probability distribution of the estimator, and chose that particle's location as the next measurement location. After choosing the next measurement location, the planner commanded the robot to move to that location.

C. Experimental Process

1. Test Environment

The experiment was conducted in a single test room with a floorplan shown in Figure 5. The ventilation system of the room was undisturbed in order to keep the test environment close to that of a typical indoor environment. Parameters of the experiment are shown in Table 3.

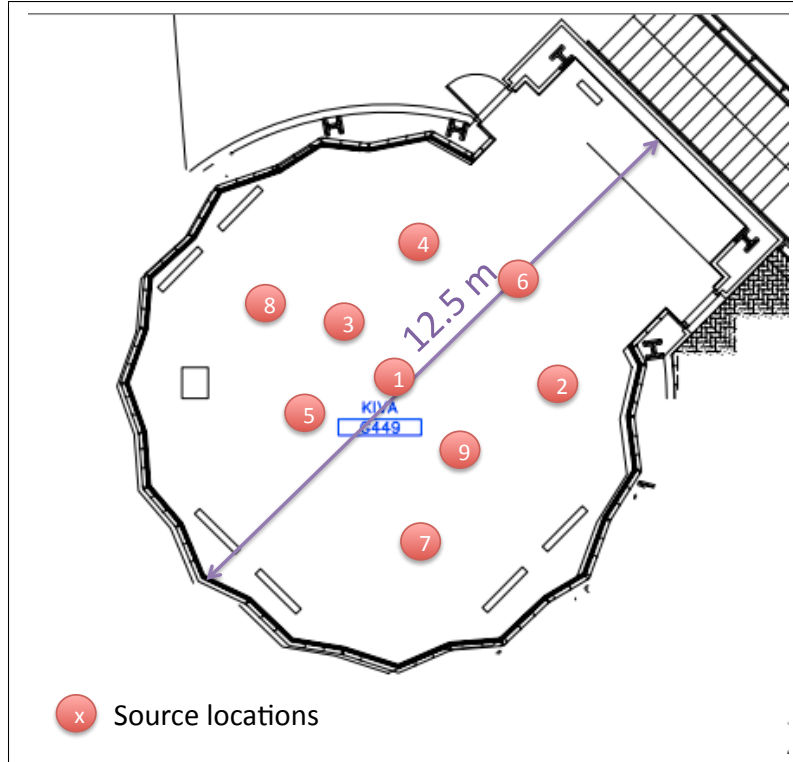


Figure 5. Testroom floorplan and chemical vapor source locations.

2. Test Procedure

A single exposed dish of ethanol was placed in the test room at least 30 minutes before the start of each trial, and remained undisturbed at its initial location for the entirety of the trial. The robot was initialized at a random location no less than 2 meters away from the location of the source, and operated autonomously throughout the trial. The duration of each trial was 35 minutes, beginning when the first chemical sensor reading was taken.

Nine sets of two trials were conducted using the nine chemical source locations shown in Figure 5. For each source location, one trial was conducted using the greedy planner, and one trial was conducted using the stochastic planner. When the location of the source was changed between trials, a waiting period of at least 2 hours was allowed, during which no ethanol was exposed. According to regulations regarding the air cycle rate for an office building, it was determined that

Table 3. Parameters of the experiment.

Chemical used as source	Liquid ethanol, 70%
Surface area of chemical vapor source	0.018 m ²
Vertical distance between sensor plane and test room floor	0.3 m
Minimum initial distance between sensor and chemical	2 m
Delay between robot start and source exposure	30 minutes
Delay between source exposure and the start of a trial	30 minutes
Duration of trial	35 minutes

the air in the test room was replaced a minimum of 4 times per hour. Thus, it was assumed that a 2 hour waiting period allowed time for the room to be cleaned of ethanol traces.

3. Data Acquisition

All of the particles of the particle filter located less than a distance of 1 meter from the true source location were considered to be within the “localization radius.” The sum of the probabilities of the particles within the localization radius at the beginning and end of each trial was used to calculate the mean localization rate achieved in that trial by the process described in section V.

The probabilities of all of the particles were logged each time the posterior was updated, and the initial and final sums of probability mass within the localization radius were calculated after the end of each trial. Raw chemical sensor readings and the robot position were also logged at a rate of 1 Hz.

V. Results

The results of this experiment contradict the hypothesis presented in section II. This section contains a summary of experimental data and detailed statistical analysis of the data to assess the hypothesis.

A. Experimental Data

For each of the nine source locations, Table 4 shows the ratio of the localization rate of a trial using the stochastic planner to the localization rate of a trial using the greedy descent planner, as well as the raw quantities used to calculate this ratio. m_0 is the initial sum of the probabilities of particle filter particles located inside the 1 meter localization radius for each trial, and m_f is the sum of the final probabilities of the same particles. The localization rate of each trial is calculated according to the equation $rate = \frac{m_f/m_0}{T_{trial}}$ where T_{trial} is the length of the trial in minutes. The ratio R is given by the equation $R = \frac{rate_{stoch}}{rate_{greedy}}$ and serves as a numerical comparison between the localization rate using the greedy planner and the localization rate using the stochastic planner for each source location.

Source Location	1	2	3	4	5	6	7	8	9
$m_{0_{greedy}}$	0.0502	0.0450	0.0500	0.0500	0.0497	0.0481	0.0493	0.0506	0.0497
$m_{f_{greedy}}$	0.0468	0.0451	0.2935	0.0511	0.0519	0.0492	0.0562	0.0503	0.0518
r_{greedy}	0.0259	0.0286	0.1656	0.0282	0.0298	0.0286	0.0303	0.0280	0.0293
$m_{0_{stoch}}$	0.0502	0.0450	0.0500	0.0500	0.0497	0.0484	0.0493	0.0506	0.0490
$m_{f_{stoch}}$	0.0521	0.0483	0.0525	0.0491	0.0480	0.0488	0.0495	0.0515	0.0491
r_{stoch}	0.0295	0.0296	0.0299	0.0279	0.0268	0.0272	0.0280	0.0285	0.0280
$R = \frac{rate_{stoch}}{rate_{greedy}}$	1.1371	1.0345	0.1807	0.9869	0.9014	0.9505	0.9251	1.0164	0.9564

Table 4. Experimental Data

The mean R_{mean} of the ratios R for the nine source locations is equal to $R_{mean} = 0.8989$ and was used to assess the hypothesis as false. The 90% confidence interval on R_{mean} is $(0.7263, 1.0714)$.

B. Statistical Hypothesis Assessment

A one-sided Student's t-test with 8 degrees of freedom on alternative hypothesis $R_{mean} > 1.2$ gave a t-statistic of -3.2466 with a corresponding p-value of 0.9941. Thus, the probability of obtaining a measured ratio greater than or equal to $R_{mean} = 0.8989$ is 99.4% under the null hypothesis ($R_{mean} = 1.2$), so the alternative hypothesis $R_{mean} > 1.2$ must be rejected. Figure 6 shows a graphical representation of the experimental data and the rejected hypothesis.

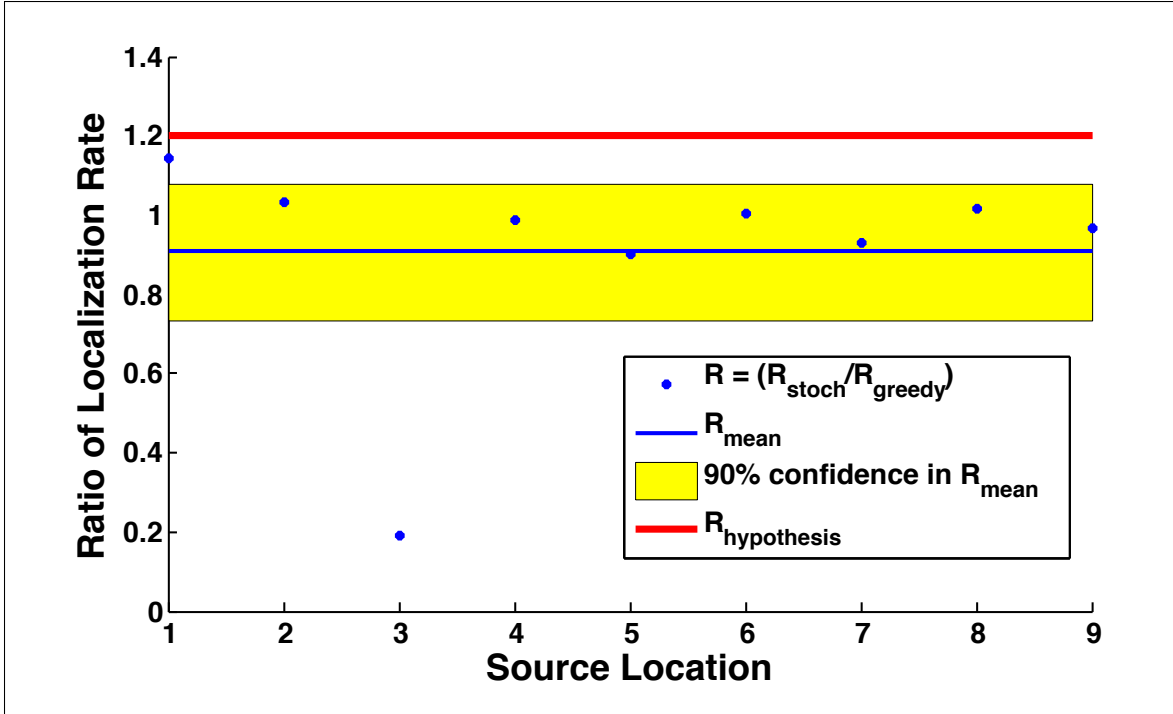


Figure 6. Graphical representation of data and hypothesis. For source location 3 the result was significantly different than for the other source locations because for source location 3 the greedy planner localized the source to a higher degree than in any of the other trials.

C. Additional Assessment of Results

In addition to the assessment of the hypothesis presented in section II, a two-sided Student's t-test with 8 degrees of freedom was used on the hypothesis $R_{\text{mean}} = 1$ to determine whether there was any statistically significant difference in the mean localization rates using the two planners. This test gave a t-statistic of -1.0903 and a p-value of 0.3073 , showing that there is no statistically significant difference in the mean localization rate achieved with the stochastic planner and the rate achieved with the simple gradient descent planner.

VI. Discussion

As described in the previous section, the stochastic planner was not shown to produce a higher mean localization rate than the simple gradient descent planner. One possible cause may have been that the system did not produce a statistically significant increase in the sum of probability mass inside the localization radius using either planner. The results of a two-sided Student's t-test on the null hypothesis $\frac{m_f}{m_0} = 1$ are given in Table 5. Although the t-statistics show some increase in the sum of probability mass inside the localization radius, particularly in the case of the stochastic planner, this increase is not significant at a 10% level.

One reason that the probability mass inside the localization radius was not shown to increase

	t-statistic	p-value
Greedy Planner	1.0296	0.3333
Stochastic Planner	1.3994	0.1993

Table 5. Student’s t-test for an increase in the sum of probability mass inside the localization radius over the time of a trial. These results show no statistically significant increase.

over the time of a trial may have been the presence of air currents in the room due to the ventilation system, the motion of the robot, and other random disturbances. Currents may have invalidated the assumption that the air directly above the true source location holds a higher chemical vapor concentration than all surrounding points. A qualitative drifting behavior was observed in carrying out the experiment, where higher concentration measurements were taken at a distance of one to two meters in one direction from the source than were taken at similar distances in other directions, and even at the exact source location. Further experimental characterization of indoor chemical dispersion is necessary to confirm this drifting behavior quantitatively. The robotic localization system tested in this experiment attempts to localize the area of highest concentration, since the estimation algorithms assume the area of highest concentration to be the location of the true source. If the true source location is in fact different from the location of the highest chemical vapor concentration, the system may not be able to accurately localize the source, regardless of which planner is used. The possibility of system failure in the manner described represents a lack of robust estimation techniques, and calls for further research in the area of estimation algorithms for indoor robotic odor localization.

The stochastic planner was expected to produce a greater localization rate than the simple gradient descent planner due to the fact that it was expected to gather concentration measurements from a larger percentage of the test room area. In experimental trials with the stochastic planner, the system did gather measurements from a larger area than in trials with the greedy planner. This result is shown qualitatively by the comparison of robot paths in Figure 7 and quantitatively in Table 6, where A_{greedy} and A_{stoch} are the percentage of the area of the test room “covered” using the greedy planner and the stochastic planner respectively. For the purpose of this analysis, the covered area is calculated by the area of the convex hull of the set of locations at which the robot took measurements, i.e., the area of the smallest convex shape that includes all of the measurement locations.

Source Location	1	2	3	4	5	6	7	8	9
A_{greedy}	0.1006	0.0750	0.237	0.0775	0.0802	0.1042	0.0669	0.0561	0.0612
A_{stoch}	0.4940	0.4523	0.5405	0.5278	0.5032	0.5717	0.4930	0.5469	0.5311

Table 6. Fraction of possible area covered by the different planning algorithms.

The differences in the area over which concentration measurements were taken using the greedy

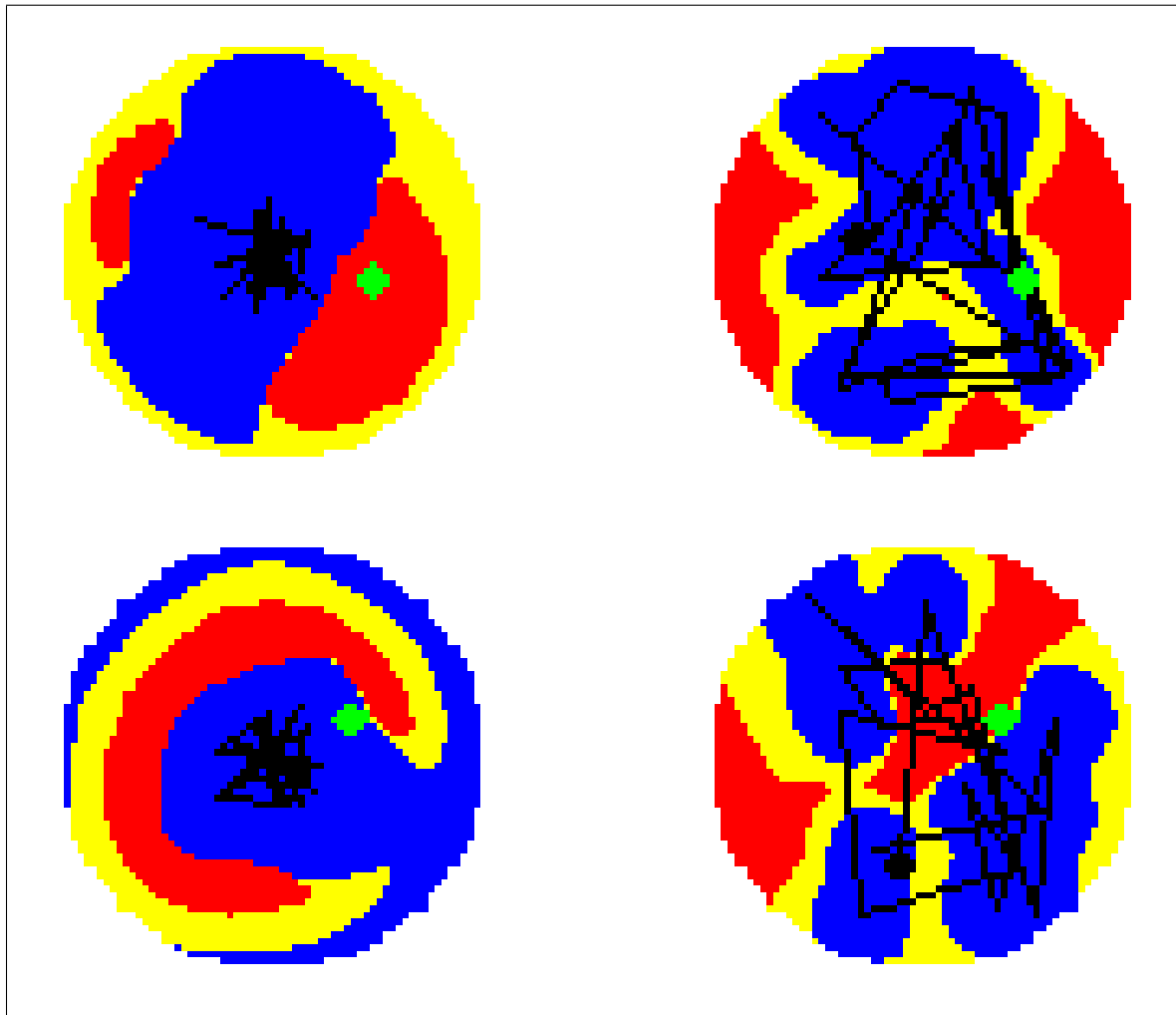


Figure 7. Comparison of robot paths and resulting final particle filter probability distributions using the greedy planner (left) and the stochastic planner (right) for source locations 7 (top) and 8 (bottom). The robot paths are shown in black, where each corner represents a measurement location, and the true source locations are shown in green. The circular color fields represent the particle filter probability distributions. The particles making up the top 25% of the probability mass is shown in red, the particles making up the next 25% are shown in yellow, and the bottom 50% are shown in blue. It is clear that the different planners produce different distributions of measurements over the space in the test room, and this results in different final particle filter probability distributions.

planner and the stochastic planner caused the two planners to produce different final particle filter probability distributions, as illustrated qualitatively in Figure 6. However, as discussed in section V, the difference in final probability distributions did not produce a statistically significant difference in the localization rate. In the case where the true source location is not the point of highest concentration, as discussed earlier in this section, the use of a localization radius about the true source location to determine the localization rate may not fully characterize differences in the performance of the two planners. Though the use of a localization radius accurately assesses the performance of the system in localizing the true source, and thus correctly and accurately assesses the hypothesis, this metric only takes into account a subset of the information gained by the particle filter during a trial.

It is feasible that a more robust estimation technique could be developed through future research that takes into account the fact that a maximum in the chemical vapor concentration field may not exist at the true source location. In this case, a preliminary analysis of the differences in performance of the greedy planner and the stochastic planner that is not entirely obscured by the assumption of a chemical concentration maximum at the true source location may prove useful. A metric that consists of calculating a weighted average distance from each particle location to the true source location was chosen. The weight of each particle was equal to the probability mass held by that particle. The weighted average distance of the final posterior of each trial from the true source location is presented in Table 7. D_{greedy} is the final weighted average distance using the greedy planner, and D_{stoch} is the final weighted average distance using the stochastic planner for each source location. The ratio $\frac{D_{stoch}}{D_{greedy}}$ is also presented as a comparison between the two planners. A two-sided Student's t-test on the hypothesis $\frac{D_{stoch}}{D_{greedy}} = 1$ gave a t-statistic of 0.8862 and a p-value of 0.4014, and thus the ratio is not statistically significantly different from 1. However, if source location 3 is ignored on grounds that the trial with the greedy planner for this location localizes the source an order of magnitude more effectively than any of the other trials, and thus dominates the results as shown in Table 4, the same test gives a t-statistic of -2.4529 and a p-value of 0.0439. This means that for the trials that seem not to localize the source, the stochastic planner may gain more information about the location of the true source than the greedy planner with statistical significance.

Source Location	1	2	3	4	5	6	7	8	9
D_{greedy}	3.0630	4.5139	2.1940	3.9041	3.8425	3.2819	3.5805	3.4443	4.0892
D_{stoch}	3.0180	4.4869	3.0832	3.9119	3.8311	3.2875	3.5517	3.4059	4.0805
$\frac{D_{stoch}}{D_{greedy}}$	0.9853	0.9940	1.4053	1.0020	0.9971	1.0017	0.9920	0.9888	0.9979

Table 7. Weighted distance of the posterior particle distribution from the true source location. The weighted distance is the average of the distances from each particle location to the source location weighted by the probability mass of the posterior held by that particle.

One non-ideal characteristic of the weighted average distance metric is that the particles far

from the true source location have a greater impact on the result than particles close to the source location. The Kullback - Leibler divergence (KL divergence) of the final estimator probability distribution from an “ideal” Gaussian posterior about the true source location for each trial is shown in Table 8. The KL-divergence metric does not allow particles far from the source to be of greater impact than particles close to the source like the weighted average distance metric does. A two-sided Student’s t-test on the hypothesis $\frac{KL_{stoch}}{KL_{greedy}} = 1$, excluding source location 3, gives a t-statistic of -0.3539 and a p-value of 0.7338. Thus, the ratio $\frac{KL_{stoch}}{KL_{greedy}}$ is not statistically significantly different from 1, even without the third source location data. This result supports the claim that the stochastic planner may be better than the greedy planner at decreasing the probability mass of particles far from the true source location. The claim makes intuitive sense since the stochastic planner allows the robot to cover more of the test room, as discussed earlier in this section. The observation that the stochastic planner may be better than the greedy planner at decreasing the probabilities of particles far from the true source location may be prove valuable in future research on robust estimation and planning techniques for robotic odor localization.

Source Location	1	2	3	4	5	6	7	8	9
KL_{greedy}	1.3819	1.8294	0.6025	1.4937	1.4636	1.3319	1.3668	1.3803	1.5682
KL_{stoch}	1.2861	1.7989	1.2882	1.5312	1.5107	1.3297	1.3736	1.3431	1.5974
Ratio $\frac{KL_{stoch}}{KL_{greedy}}$	0.9306	0.9833	2.1381	1.0251	1.0322	0.9984	1.0050	0.9730	1.0186

Table 8. Kullback-Leibler divergence of the final particle filter posterior distribution from an ‘ideal’ Gaussian posterior distribution .

A. Future Work

As discussed in section VI, one reason that the experimental results did not show a statistically significant difference in the localization rates using the greedy planner and the stochastic planner was the lack of statistically significant difference between final and initial sums of probability mass within the localization radius. The suspected cause of this lack of difference is the use of an inadequate estimation technique. It is believed that further research in the area of probabilistic estimation for robotic odor localization is necessary before additional research in the area of planners using the formulation of this experiment will be meaningful.

There are many possible ways to improve estimation. The simplest involves simply updating the parameters of the current estimator with more informed values. The data collected while running the trials required of this experiment forms a much larger dataset than the preliminary set used to fit parameter values for the measurement model described in section B, and could be used to improve the measurement model. Additionally, the value for the measurement noise, σ in Table 1, was set to a value an order of magnitude larger than the value indicated by the fitting of preliminary data for this experiment, because in preliminary trials this σ value caused the probability estimate to collapse to a point that was not the true source location. As shown in Table 5, the

probability mass inside the localization radius did not change in a statistically significant manner over the course of the trials, meaning that the posterior estimate may have been too slow in collapsing. Setting the measurement noise to a smaller value would cause the posterior to collapse more quickly, which may result in a larger change in the sum of probability mass inside the localization radius over the course of a trial.

Rigorous characterization of the sensor dynamics could also help with the development of a more capable estimator. As noted in section B, the baseline value of sensor readings changed significantly from one test day to another. Understanding and accounting for the factors that caused the changes in baseline readings could improve the measurement model. It was also qualitatively observed that the sensor readings took more time to stabilize when subjected to a concentration that decreased over time than they took to stabilize when subjected to an increasing chemical concentration. Understanding and characterizing time constants associated with this asymptotic behavior, as well as other higher frequency dynamics, may be another way to improve estimator performance. Finally, an accurate mapping from sensor readings to chemical concentrations may be necessary for more sophisticated measurement models. Raw sensor readings have units of Ohms, and it was deemed unnecessary to characterize the exact mapping to units of parts per million in this experiment, due to the simplicity of the chosen measurement model. An exact mapping could be experimentally determined by recording sensor readings over time while exposing the sensor to a known concentration of ethanol in a small, sealed container.

The characterization and mitigation of indoor chemical vapor dispersion dynamics holds the broadest range of possibilities for improvements in estimation technique. The likelihood function used by the estimator in this experiment is based on a model of diffusion as presented in section B, but as discussed in Section III, the effects of convection and other air currents may dominate the effect of diffusion for chemical dispersion in an indoor environment. There are many ways to incorporate convective effects into the measurement function, covering a large range in their degree of complexity. The most accurate description of the behavior of the dispersing chemical would likely require methods of computational fluid dynamics dependent on knowledge of the room shape and ventilation characteristics. These computations, however, may be too resource intensive to run in real-time on a robotic platform, and the dependence on location specific features potentially causes the generality of the solution to be lost. The latter objection could be addressed by integrating the dispersion model with online mapping, but this would greatly increase the complexity of the solution. It may be wise to exhaust simpler options before turning to the integration of computational fluid dynamics tools to improve the estimator.

Probabilistically motivated models similar to the model assumed in this experiment may still be able to reflect the fact that convection may be the dominant dispersive effect. For instance, if convection is dominant, the dispersion may be characterized by small pockets of high concentration, with these pockets more common and dense near the source than at the edges of a test room.

This would lead to a higher variance set of readings near the source location, where many high-concentration packets quickly pass over the inlet of the sensor, than at the edge of the test room, where packets may be less common and their concentration may be lower than the concentration of packets near the source. This variation in variance of the readings over distance from the source was observed qualitatively in this experiment, as well as by Ferri et. al. [2] Thus, incorporating the variance of concentration readings in addition to the average value of the readings may result in an effective estimation technique.

VII. Summary and Conclusion

The data collected does not contain statistically significant evidence that a stochastic planner localizes a chemical source at a faster rate than a greedy gradient descent planner. It is believed that any potential difference in the performance of the planning algorithms was masked by inadequacy of the estimation techniques used in this experiment. Further research into robust estimation techniques for indoor robotic odor localization is needed.

VIII. Acknowledgments

We, the authors, would like to thank our faculty advisors, Professors Youssef Marzouk and Nicholas Roy, for the expertise and experience they brought to the project, and all the time they invested in teaching us and brainstorming with us. We would like to thank Josh Joseph and Javier Velez for always being happy to make time to help us work through the issues we faced, and for being so patient and understanding while explaining new concepts and techniques to us. Xun Huan and Sachi Hemachandra also volunteered their time to help us progress through the project. Finally, we must thank the 16.62x course staff: Professors Brian Wardle, Edward Greiter, and Sheila Widnall, communications instructor Jennifer Craig, laboratory instructors Dick Perdichizzi, Dave Robertson, and Tod Billings, and teaching assistant Louis Perna. The course staff was determined to help us successfully complete our project, and help push us through to the finish line. Without the guidance of all those who helped us on this project, we would have never have been able to complete it.

References

- [1] Kowadlo, G. and Russell, R. A., "Robot Odor Localization: A Taxonomy and Survey," *The International Journal of Robotics Research*, Vol. 27, No. 8, 2008, pp. 869–894.
- [2] Ferri, G., Caselli, E., Mattoli, V., Mondini, A., Mazzolai, B., and Dario, P., "SPIRAL: A novel biologically-inspired algorithm for gas/odor source localization in an indoor environment with no strong airflow," *Robotics and Autonomous Systems*, Vol. 57, No. 4, 2009, pp. 393 – 402.
- [3] Bergman, N., "Recursive Bayesian Estimation," *Department of Electrical Engineering, Linköping University, Linköping Studies in Science and Technology. Doctoral dissertation*, , No. 579, 1999.
- [4] Bottou, L., "Stochastic gradient learning in neural networks," *Proceedings of Neuro-Nimes*, Vol. 91, 1991.
- [5] Maskell, S. and Gordon, N., "A tutorial on particle filters for on-line nonlinear/non-Gaussian Bayesian tracking," *Target Tracking: Algorithms and Applications (Ref. No. 2001/174)*, IEE, IET, 2001, pp. 2–1.
- [6] Ishida, H., Tanaka, H., Taniguchi, H., and Moriizumi, T., "Mobile robot navigation using vision and olfaction to search for a gas/odor source," *Autonomous Robots*, Vol. 20, 2006, pp. 231–238, 10.1007/s10514-006-7100-5.
- [7] Borman, S., "The Expectation Maximization Algorithm: A short tutorial," http://www.seanborman.com/publications/EM_algorithm.pdf.
- [8] Baird, L. and Moore, A., "Gradient descent for general reinforcement learning," *Proceedings of the 1998 conference on Advances in neural information processing systems II*, MIT Press, Cambridge, MA, USA, 1999, pp. 968–974.
- [9] Posner, J., Buchanan, C., and Dunn-Rankin, D., "Measurement and prediction of indoor air flow in a model room," *Energy and Buildings*, Vol. 35, No. 5, 2003, pp. 515 – 526.
- [10] Lilienthal, A., Zell, A., Wandel, M., and Weimar, U., "Sensing odour sources in indoor environments without a constant airflow by a mobile robot," *Robotics and Automation, 2001. Proceedings 2001 ICRA. IEEE International Conference on*, Vol. 4, 2001, pp. 4005 – 4010 vol.4.
- [11] Russell, R., "Robotic location of underground chemical sources," *Robotica*, Vol. 22, No. 01, 2004, pp. 109–115.

A. Additional Figures

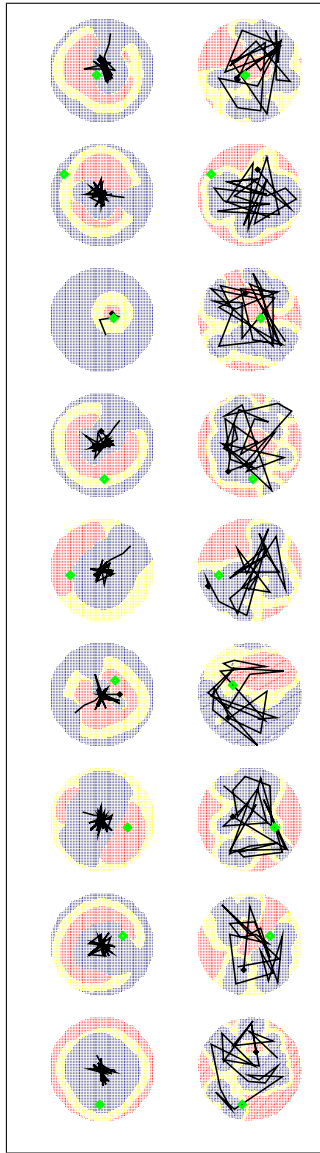


Figure 8. Robot paths and resulting final posterior probability estimates using the greedy planner (left) and the stochastic planner (right) for all source locations, with source location 1 at the top and source location 9 at the bottom. The robot paths are shown in black, where each corner represents a measurement location, and the true source locations are shown in green. The circular color fields represent the particle filter probability distributions. The particles making up the top 25% of the probability mass is shown in red, the particles making up the next 25% are shown in yellow, and the bottom 50% are shown in blue.